Study of helium bubble evolution in highly neutron-irradiated beryllium by using x-ray micro-tomography and metallography methods

2011 Phys. Scr. 2011 014012

(http://iopscience.iop.org/1402-4896/2011/T145/014012)

Phys. Scr. **T145** (2011) 014012 (6pp) doi:10.1088/0031-8949/2011/T145/014012

Study of helium bubble evolution in highly neutron-irradiated beryllium by using x-ray micro-tomography and metallography methods

V Chakin[1], R Rolli[1], A Moeslang[1], P Kurinskiy[1], P Vladimirov[1], C Ferrero[2], R Pieritz[2] and W Van Renterghem[3]

[1] Karlsruhe Institute of Technology (KIT), Institute for Applied Materials, PO Box 3640, D-76021 Karlsruhe, Germany
[2] European Synchrotron Radiation Facility, PO Box 220, F-38043 Grenoble Cedex, France
[3] SCK•CEN, Boeretang 200, B-2400 Mol, Belgium

E-mail: vladimir.chakin@kit.edu

Received 10 May 2011
Accepted for publication 9 August 2011
Published 16 December 2011
Online at stacks.iop.org/PhysScr/T145/014012

Abstract
Beryllium will be used as a plasma-facing material and a neutron multiplier in fusion reactors. The processes of helium accumulation in fusion and fission reactors are similar. Therefore, it is possible to extrapolate the data obtained on beryllium irradiated in a fission reactor to a fusion one. Fragments of the beryllium matrix of the BR2 reactor irradiated at 323 K up to a fast neutron fluence of 4.67×10^{22} cm^{-2} (E >1 MeV) and helium accumulation of about 22 500 appm with additional annealing at 1123 and 1273 K for 0.5, 1. 5 and 10 h were used for the investigation of helium porosity by optical metallography and x-ray micro-tomography methods. The possibility of using the XRT method for investigations of helium porosity evolution in irradiated and annealed beryllium was demonstrated. The non-uniformity of helium bubble formation in the material leads to a non-homogeneous swelling observed on the cross-section of the beryllium samples. The reason for high swelling in the bulk of the beryllium sample could be the formation of large stable helium bubbles, which are not mobile and not mutually connected.

PACS numbers: 28.52.Fa, 61.80.Hg, 28.41.Pa

(Some figures may appear in colour only in the online journal)

1. Introduction

Beryllium will be used as a plasma-facing material of a first wall and a neutron multiplier of a test blanket module in ITER, and as a neutron multiplier in the European Helium Cooled Pebble Bed (HCPB) DEMO blanket. Under neutron irradiation, beryllium accumulates helium atoms due to nuclear threshold reactions with high-energy neutrons. The helium accumulation directly depends on neutron fluence and leads to swelling and other negative radiation effects in beryllium which could limit the lifetime of the fusion reactor components. At present, beryllium is widely used as a neutron reflector or a moderator in research nuclear reactors. The main characteristics of the beryllium used in research reactors are low operation temperature (323–343 K) and a high neutron dose accumulation to the end-of-life of the beryllium blocks. It seems very attractive to use fragments of the irradiated beryllium blocks followed by high-temperature annealing tests for reproducing fusion reactor conditions. In this work, the fragments of the BR2 reactor beryllium matrix were investigated by optical metallography (OM) and x-ray micro-tomography (XRT) methods. The obtained results are discussed and summarized as a model describing the evolution of pores and helium bubbles in low-temperature irradiated beryllium depending on annealing parameters.

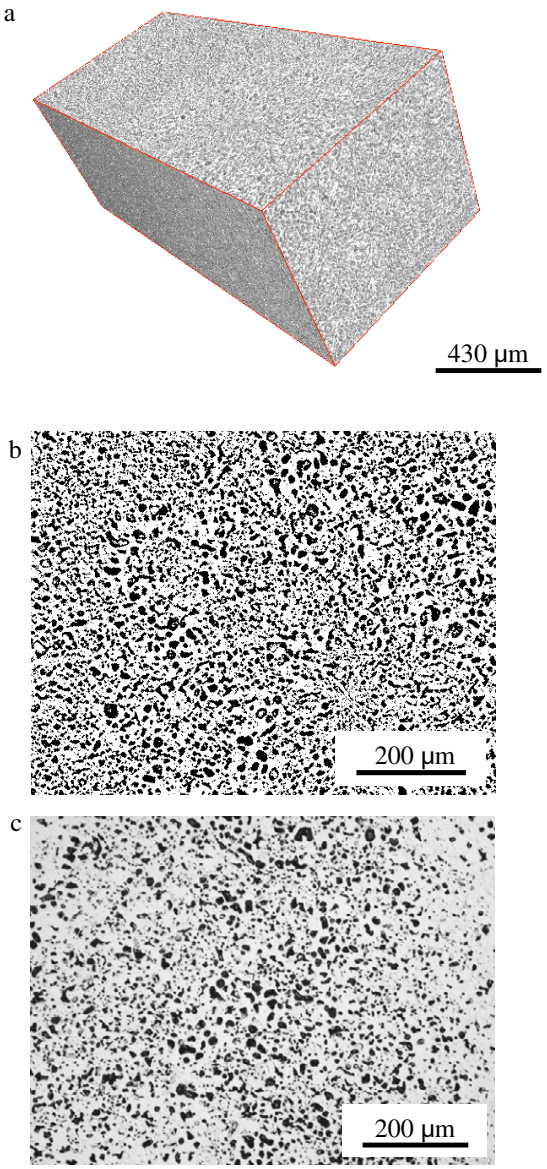

Figure 1. Images of irradiated beryllium annealed at 1273 K for 5 h: ROI (a) and cross sections obtained by XRT (b) and by OM (c) methods.

2. Experimental details

Irregular-shaped samples with characteristic sizes of about 1 mm used in this work were prepared from fragments of the beryllium matrix of the BR2 nuclear reactor located at SCK•CEN, Belgium. The original material is S-200E beryllium grade produced by Brush Wellman Inc., USA, which contains in wt.% < 2.0 BeO, < 0.18 Fe, < 0.15 C, < 0.15 Al, < 0.08 Mg, < 0.08 Si and < 0.04 of each of the other metallic elements. The average grain size was in the range 10–13 μm [1]. The beryllium matrix was operating at a temperature of about 323 K for 15 years, which resulted in a fast neutron fluence ($E > 1$ MeV) of 4.67×10^{22} cm^{-2} and helium accumulation of about 22 500 appm. Irradiated beryllium samples were annealed at 1123 and 1273 K for 0.5, 1, 5 and 10 h in vacuum. Prepared beryllium samples were investigated at KIT by an optical microscope, Olympus GX51, placed in a glove box. Preparation of the sample surfaces was performed under argon atmosphere. The optical

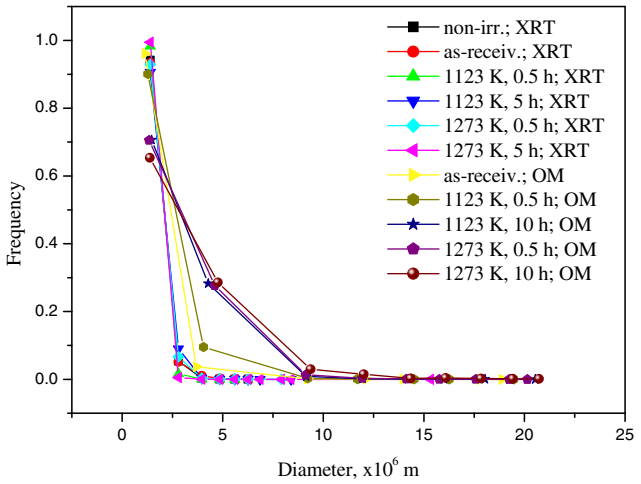

Figure 2. Frequency of pore diameters in the bulk of irradiated beryllium samples based on XRT and OM measurements.

microscope images were subjected to further analysis using the method from [2]. The Feret diameters of pores and bubbles were measured by their areas. Most pores appear to have smaller sizes than their actual dimensions since not all pores are sectioned through their maximum diameters. Taking into account this effect, an appropriate correction from two-dimensional (2D) pore distribution to 3D volumetric distribution was performed. Using corrected size distribution and calculated values of the average pore diameter, swelling of different sample regions was evaluated.

The irradiated beryllium samples were also investigated by the XRT at the European Synchrotron Radiation Facility, Grenoble, France [3, 4]. The high-resolution micro-tomography setup at the ID19 beamline used for the experiment has a monochromatic x-ray beam of energy in the range 7–11 keV. The beryllium samples were scanned with a spatial resolution of 1.4 μm. The method after 3D reconstruction of the obtained data allows us to obtain the pore (bubble) diameters and volumetric distribution.

3. Results and discussion

3.1. Measurements of pore distributions

XRT seems to be an attractive method for post-irradiation examinations of irradiated materials, which can be used in parallel with the common OM. It should be noted that one needs to establish points of accordance and limitations for successful application of XRT for the purposes of radiation material science. One possibility is to use XRT for the investigation of pores or bubbles formed in microstructure of irradiated beryllium. It is necessary to extract region of interest (ROI) from the bulk of all data after scanning the sample by XRT. The ROI has a volume of about 10^{-10}–10^{-12} m^3 and characterizes a middle volume state of the scanned microstructure. In contrast with the XRT method, OM gives data from a definite 2D cross-section of the sample (i.e. with an exact location of the selected area of the sample for the investigation). The use of a correction of pore diameters and distributions for the truncation effect and recalculation from the 2D to 3D volumetric distribution offers

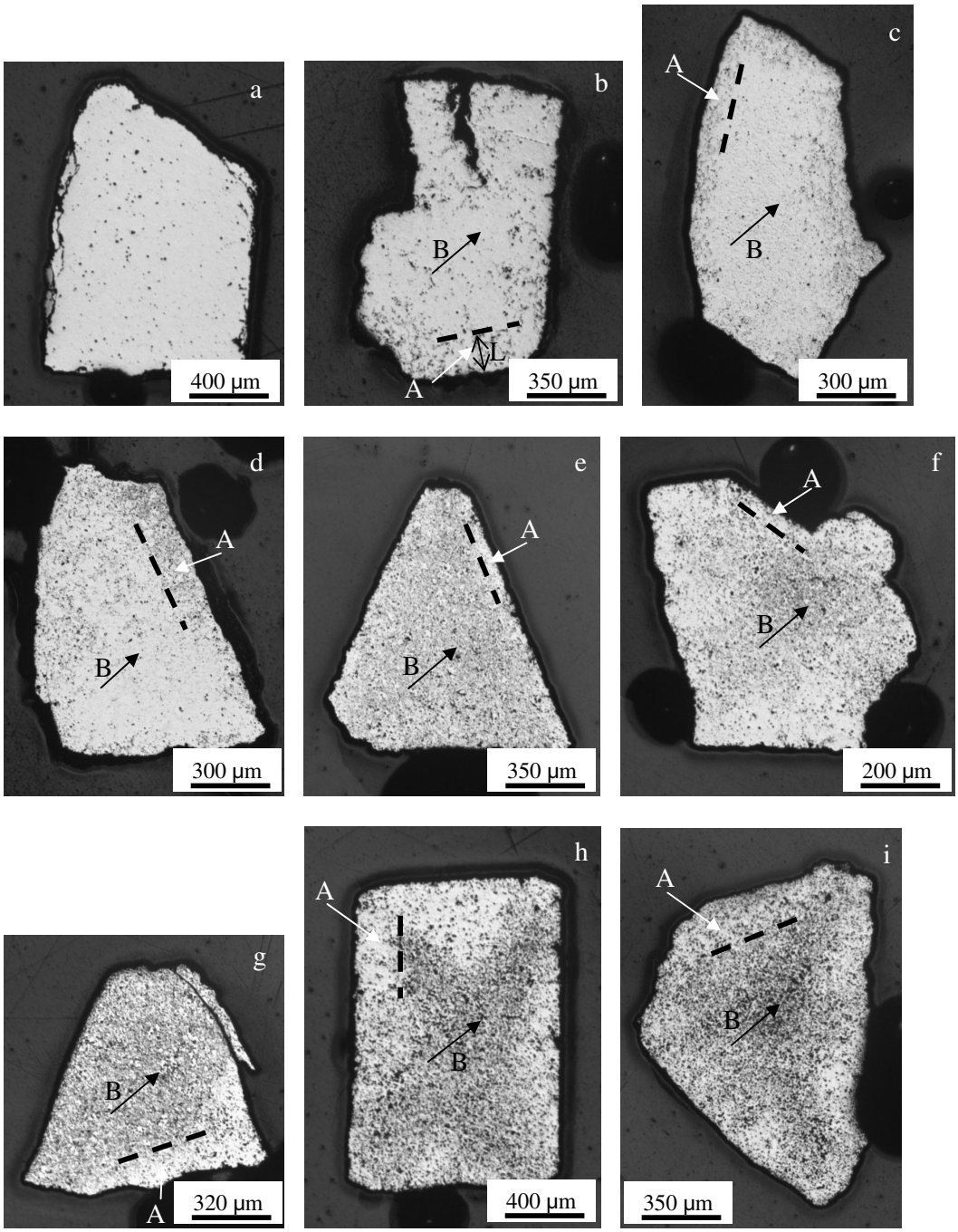

Figure 3. Optical images of irradiated beryllium samples as-received (a), annealed at 1123 K for 0.5 h (b), 1 h (c), 5 h (d), 10 h (e) and at 1273 K for 0.5 h (f), 1 h (g), 5 h (h) and 10 h (i). Different dimensions and distributions of pores and gas bubbles in regions to the surface (marked A) and in the bulk of the samples (marked B).

a possibility of characterizing the state of microstructure within a selected sample volume. Figure 1 shows an example of processed ROI for irradiated beryllium annealed at 1273 K for 5 h (see figure 1(a)) and cross-sections obtained by XRT (see figure 1(b)) and by OM (see figure 1(c)) methods. Despite the different principles of the image formation by XRT and OM, very similar images were formed by both methods. In particular, the main features of the XRT and OM images such as a non-uniform distribution of pores, quite similar pore diameters and so on are similar for both the methods. This means that it is possible to use the method of XRT for the study of pore distribution in irradiated beryllium. Figure 2 represents a function of pore distribution (as frequency of availability in the beryllium microstructure) on their diameters obtained by XRT and OM. The 3D OM pore distribution was calculated for a volume of the beryllium sample bulk that allows comparison between data obtained by XRT and OM. In principle, the pore diameter frequencies obtained by XRT and OM are in good correlation for both annealed and initial states. Some differences may have only the order of the pore diameter extraction from the XRT data after the sample scanning for this figure. In particular, a selection with comparatively dense subdivision by pore diameters was made in the case of the use of the XRT method. This gave the difference between pore diameter frequencies for XRT and OM for diameters from 3×10^{-6} up to 9×10^{-6} m. It is clear

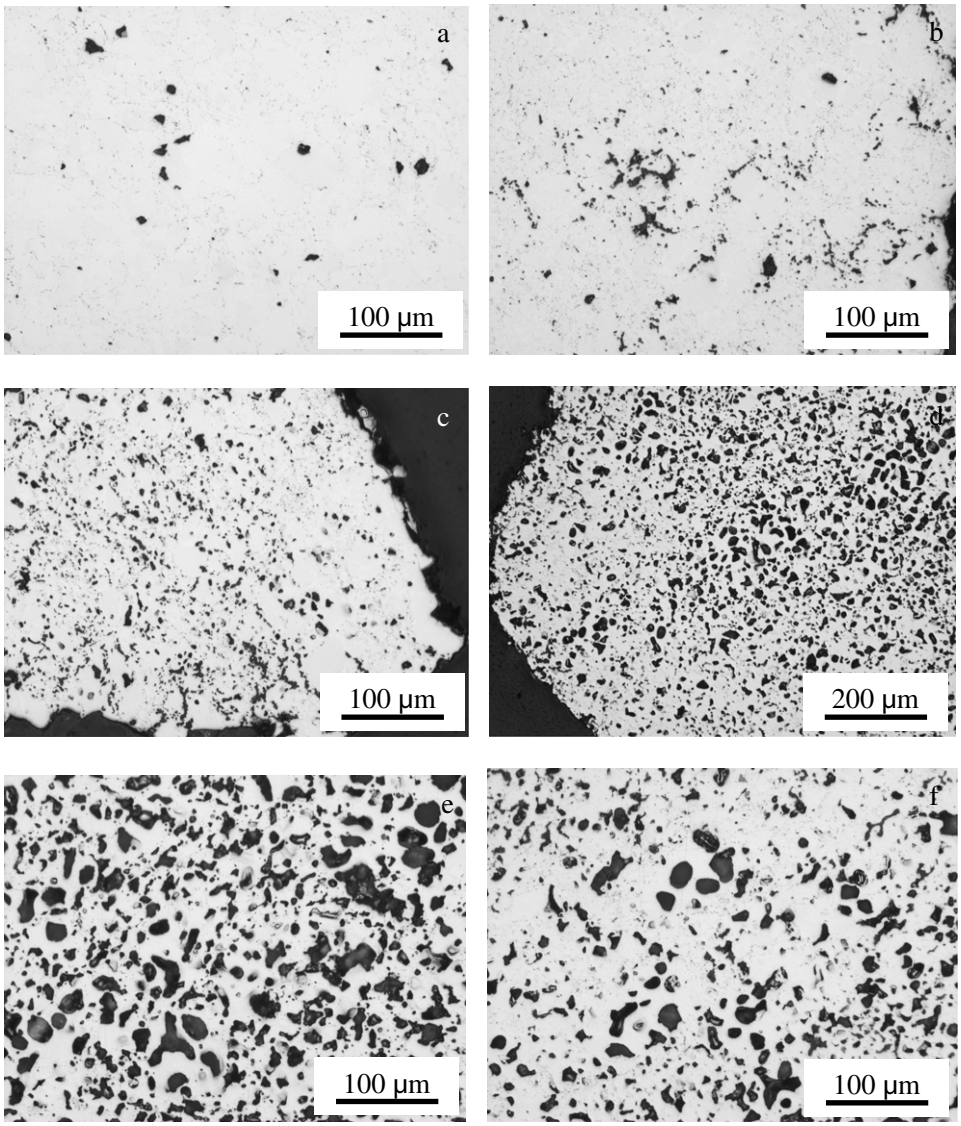

Figure 4. Optical images of pores and gas bubbles in the beryllium samples: (a) as-received, bulk; (b) annealed at 1123 K for 0.5 h, to the surface; (c) annealed at 1123 K for 10 h, to the surface; (d) annealed at 1273 K for 10 h, both in the bulk and to the surface; (e) annealed at 1273 K for 10 h, bulk; (f) annealed at 1273 K for 10 h, to the surface.

that most of the pores in irradiated and annealed beryllium have an average diameter not exceeding 4–5 $\times$ 10^{-6} m with its maximum location in the range 1–2 $\times$ 10^{-6} m.

3.2. Swelling

The theory of swelling and helium release for reactor materials was in principle proposed by Barnes [5] and later developed for beryllium in [6, 7]. It is clear that parameters of helium pores or bubbles define beryllium swelling values. The swelling of irradiated beryllium samples was evaluated by geometrical size measurements [8] or calculated by the use of OM or SEM images [1]. These measurements and calculations give average swelling values for the entire sample volume not taking into account possible local non-uniformity of swelling. Figure 3 shows OM images of irradiated beryllium annealed at high temperatures. The obtained images allow the observation of non-homogeneous pore distribution while comparing the central parts (bulk, marked as B on the images, B-region) with regions close to the external surface (marked as A, A-region). Only the sample in the as-received state does not possess non-uniformity between A- and B-regions (figure 3(a)). The widths of the A-regions depend on the parameters of annealing. In particular, at the lowest parameters of annealing (figures 3(b)–(d)) A-regions are enriched with pores when compared to B-regions. However, at higher parameters of annealing (figures 3(e)–(i)) the reverse situation occurs, i.e. the A-regions appear to be pore-depleted zones. The calculated local swelling values for both A- and B-regions of all investigated samples are shown in table 1. As-received beryllium exhibits no significant swelling. With increasing annealing temperature and time, the beryllium swelling increases for both A- and B-regions at different rates. Until annealing at 1123 K for 5 h, the A-regions have higher swelling than the B-regions. This effect can be caused by the influence of vacancy flux on the redistribution of helium atoms which is directed from the surface towards the material bulk. For helium atoms two possible routes are available to reach the external surface. One route is diffusion from the grain body to boundaries and along them towards the

Table 1. Swelling of beryllium samples.

Characteristics of samples	Swelling (%)	
	Bulk	To surface
Irradiated	2.2	2.2
Irr., ann. 1123 K, 0.5 h	2.8	8.9
Irr., ann. 1123 K, 1 h	2.1	20.0
Irr., ann. 1123 K, 5 h	8.8	11.0
Irr., ann. 1123 K, 10 h	52.0	12.2
Irr., ann. 1273 K, 0.5 h	36.3	4.6
Irr., ann. 1273 K, 1 h	71.2	6.6
Irr., ann. 1273 K, 5 h	77.3	21.2
Irr., ann. 1273 K, 10 h	193.9	23.3

surface. The other one is direct diffusion to the surface through opposite direction flux of vacancies (the Kirkendall effect). In both cases of helium atom diffusion, bubble formation can occur preferably on the grain boundaries as well as in a grain matrix with the formation of helium–vacancy stable complexes. Vacancies reach the central part of the sample only after 5 h of annealing at 1123 K when the swelling starts to increase significantly in the B-region. At higher annealing parameters, vacancies already free reach the bulk and provoke the intensive processes of helium bubble formation in the entire volume of the sample. As a result, the swelling in the B-regions increases up to extremely high values. In particular, for maximal annealing parameters the swelling reaches values of more than 190%. No data showing such a high swelling value for neutron-irradiated beryllium are found in the literature [1, 9, 10]. In the A-regions the swelling values are comparatively lower than those for the B-regions for the sample annealed at 1123 K for 10 h. For these high-temperature parameters of annealing, an accelerated helium release outside the samples during the annealings occurs. Certainly, the maximal release takes place from regions that are closer to the surface. The possible mechanisms of release can be both the diffusion of single helium atoms to the surface and the motion of helium bubbles mainly along grain boundaries. In [1, 11], the release of part of the helium from irradiated beryllium under annealing has been established.

Figure 4 presents the morphology and distribution of helium pores and bubbles in irradiated beryllium in detail. The as-received state (figure 4(a)) is characterized by the presence of pores with an irregular form distributed uniformly on the microstructure. The bubble growth with the formation of bubble chains along the grain boundaries takes place in the A-region after annealing at minimal parameters (1123 K for 0.5 h; figure 4(b)). At higher parameters of annealing (figure 4(c)) the A-region is already transformed from the bubble-enriched zone to the depleted zone since the helium release outside the sample is continued at a higher speed. The most interesting changes in beryllium microstructure were observed after annealing at the highest parameters (1273 K for 10 h, figure 4(d)). A great difference between A- and B-regions in swelling values is found (see table 1). This could mean that the formation of the stable helium bubbles with large sizes in the B-region takes place (figure 4(e)). These large bubbles are not mobile and not connected with each other since the high rate of swelling is impossible in the case of the formation of open porosity [12, 13]. These bubbles

Table 2. Calculated diffusion coefficients of He in Be and self-diffusion coefficients of Be.

Parameters of annealing	Diffusion coefficient of He in Be, D_{He} ($\times 10^8$ cm^2 s^{-1})	Self-diffusion coefficient of Be, D_{Be} ($\times 10^8$ cm^2 s^{-1})
1123 K, 0.5 h	15	1.3
1123 K, 1 h	5.3	
1123 K, 5 h	1.1	
1123 K, 10 h	0.18	
1273 K, 0.5 h	4.7	9.9
1273 K, 1 h	4.2	
1273 K, 5 h	2.6	
1273 K, 10 h	3.6	

have sizes up to 6×10^{-7} m and are located without visible attachment to the grain boundaries. The depleted zones around large bubbles were formed because the large volumes play the role of a sink for point defects including helium atoms. Due to the presence of a high-vacancy flux directed from the external surface, permanent coalescence of the bubbles takes place. Similar large bubbles are also formed in the A-region (figure 4(f)), while helium release occurs caused by the diffusion of small bubbles towards the external surface.

3.3. Diffusion coefficients

Using the data from figure 3, effective diffusion coefficients of helium D_{He} in beryllium for the annealing parameters were calculated and compared with the literature self-diffusion coefficients of beryllium D_{Be} [14, 15] (see table 2). The calculations of the effective diffusion coefficients D_{He} were performed using the equation

$$D_{He} = L^2/t,$$

where L is the diffusion path from the external surface to the black broken line, which can be measured on figure 3 for each annealing parameter (see figure 3(b) as an example) and t is the exposure to annealing. The performed calculations are approximate because it is quite difficult to measure with a high accuracy the diffusion paths on the OM images. Actually, this calculation results in a superposition of two diffusion objects—vacancies and helium atoms (or their small complexes or bubbles). For example, for annealing tests at 1273 K D_{He} is systematically less than D_{Be}, which illustrates comparatively small input of vacancies (because the diffusion coefficient for vacancies is equal to the self-diffusion coefficient for crystals) to the resulting effective diffusion coefficients.

4. Conclusion

Samples of the beryllium matrix of the BR2 reactor, irradiated at 323 K up to fast neutron fluence of 4.67×10^{22} cm^{-2} ($E > 1$ MeV) and helium accumulation of about 22 500 appm, were investigated using the OM and XRT methods. Irradiated beryllium samples were annealed at 1123 and 1273 K for 0.5, 1, 5 and 10 h in vacuum. Good correlation between the pore diameter frequencies obtained by XRT and OM methods was seen, which allowed the use of the XRT method for porosity analysis in irradiated beryllium.

High-temperature annealing tests in vacuum caused redistribution of helium atoms in the beryllium microstructure under the strong influence of vacancy flux from the external surface towards material bulk. As a result, the non-uniformity of helium bubble formation in the bulk and close to the surface regions takes place. This effect, accordingly, leads to a high non-uniformity of swelling for the bulk and surface regions. The reason for high swelling in the bulk of annealed beryllium samples could be the formation of large stable helium bubbles, which are not mobile and not mutually connected.

References

[1] Leenaers A *et al* 2008 *J. Nucl. Mater.* **372** 256
[2] Huang K-P and Form W 1990 *Prakt. Metallogr.* **27** 332
[3] Rabaglino E *et al* 2003 *Nucl. Instrum. Methods Phys. Res.* B **200** 352
[4] Moeslang A *et al* 2009 *J. Nucl. Mater.* **386–388** 1052
[5] Barnes R S 1964 *J. Nucl. Mater.* **11** 135
[6] Dubinko V I and Barabash V R 1995 *J. Nucl. Mater.* **225** 22
[7] Rabaglino E, Ronchi C and Cardella A 2003 *Fusion Eng. Des.* **69** 455
[8] Chakin V P, Kupriyanov I B and Melder R R 2004 *J. Nucl. Mater.* **329–333** 1347
[9] Sernyaev G A 2001 *Radiation Damageability of Beryllium* (Ekaterinburg: Ekaterinburg Publishers) p 256
[10] Chakin V P 1999 *Phys. Met. Metallogr.* **88** 200
[11] Chakin V *et al* 2011 *J. Nucl. Mater.* **416** 3
[12] Scaffidi-Argentina F 2001 *Fusion Eng. Des.* **58/59** 641
[13] Rabaglino EJ. *et al* 2002 *Nucl. Mater.* **307–311** 1424
[14] Smithells C I 1976 *Metals Reference Book* (Oxford: Butterworth)
[15] Goltsev V P, Chechetkina Z I and Sernyaev G A 1977 *Radiation Material Science of Beryllium* (Minsk: Science and Technique Publishers) (in Russian)